ACS Catalysis

LETTER

pubs.acs.org/acscatalysis

Overcoming the Strong Metal−Support Interaction State: CO Oxidation on TiO_2(110)-Supported Pt Nanoclusters

Simon Bonanni, Kamel Aït-Mansour,* Harald Brune, and Wolfgang Harbich

Institute of Condensed Matter Physics, Ecole Polytechnique Fédérale de Lausanne (EPFL), CH-1015 Lausanne, Switzerland

Supporting Information

ABSTRACT: We combine low-temperature scanning tunneling microscopy and measurements of the catalytic activity to establish a structure−reactivity correlation for the CO oxidation on Pt nanoclusters on rutile TiO_2(110)-(1 × 1). Annealing of the clusters to 1100 K leads to their encapsulation by a reduced titania layer. We present a method how this catalytically passive strong metal−support interaction state can be transformed into a very active one. We believe that our method is of general interest well beyond the presented system.

KEYWORDS: strong metal−support interaction (SMSI), Pt nanoclusters, TiO_2, catalysis, CO oxidation, scanning tunneling microscopy (STM)

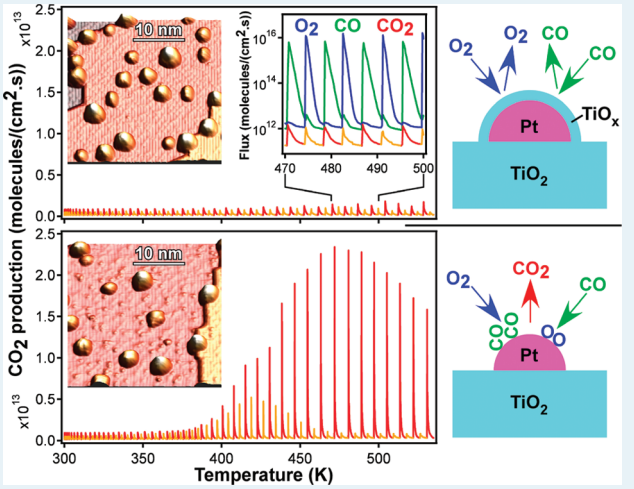

Metal clusters supported on metal oxide surfaces are currently intensively studied as model catalysts to achieve an atomic scale understanding of nanocatalysis.[1,2] Size, crystal structure, chemical composition, and electronic properties of the metal clusters can strongly influence their catalytic activity.[3,4] For instance, the surface of bulk Au is well-known to be catalytically inactive, whereas dispersed Au nanoparticles on oxides exhibit a high catalytic activity for various chemical reactions, for example, for low-temperature CO oxidation.[5−13] Electron charging of Au clusters bound to MgO(001) surface defects strongly influences CO adsorption[14] and CO oxidation.[15−18] In contrast to Au, bulk Pt is known to be an excellent catalyst for a number of reactions, including CO oxidation,[19,20] which justifies its wide use in current industrial catalysts.

However, nanoparticles of Pt, as well as of other group 8−10 noble metals, on TiO_2 lose their H_2 and CO chemisorption capacity when annealed above 700 K.[21] This effect is attributed to a "strong metal-support interaction"[21] (SMSI); the passive state is commonly referred to as the SMSI state.[22−50] Since it severely restricts the practical use of the catalyst, this state has been studied intensively over the last three decades by means of surface-sensitive techniques and for several metals (Pt, Pd, Rh, etc.) on atomically well-defined oxide surfaces such as TiO_2-(110), Fe_3O_4(111), and CeO_2(111), revealing in all cases that the SMSI state is related to an encapsulation of the deposited metal by a reduced thin oxide layer coming from the support during annealing.[24−50] This encapsulation is found to be the cause of the strong decrease in the metal's capacity to adsorb CO.[24−32]

Here, we report on a method to remove the SMSI state for Pt nanoclusters on rutile TiO_2(110)-(1 × 1). We use an ultrahigh vacuum experimental setup[51] combining low-temperature scanning tunneling microscopy (STM)[52] and catalytic measurements. Suboxide-encapsulated Pt clusters are found to be almost inactive in catalytic CO oxidation. As we will show, this SMSI state can be transferred into a very active and thermally stable one, thus overcoming the SMSI limitation.

Figure 1 shows STM images of 25% monolayer (ML) of Pt (1 ML Pt is defined as the Pt(111) atomic surface density = 1.5 × 10^{15} atoms/cm^2) deposited at room temperature on a clean rutile TiO_2(110)-(1 × 1) surface,[53] followed by annealing at 1100 K for 3 h (see the Supporting Information). The overview STM image shows regularly dispersed Pt clusters that appear as bright spots. Images taken at many other locations are very similar and thus reveal that the sample morphology is quite homogeneous, such that spatially integrating catalytic reaction measurements based on mass spectroscopy can safely be related to the shown cluster morphology. The close-up STM image (Figure 1b) shows that the Pt clusters have different apparent sizes and have grown on the bare terraces as well as at the monatomic steps of the TiO_2(110) surface. The bright and dark

Received: January 5, 2011
Revised: February 15, 2011
Published: March 04, 2011

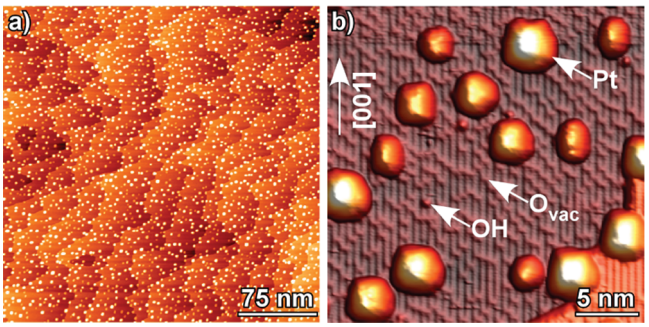

Figure 1. (a) Overview and (b) close-up STM images of 25% ML Pt deposited at room temperature on $TiO_2(110)$-(1 × 1) followed by annealing at 1100 K for 3 h (+1.5 V, 0.1 nA, 80 K).

lines resolved on the bare terraces correspond to [001]-oriented rows of 5-fold-coordinated Ti and bridging O atoms, respectively.[53] In addition, we discern by their apparent heights two types of bright point defects randomly distributed on the oxygen rows. The majority are O vacancies (O_{vac}) appearing with a height of 0.3 Å, and the minority are hydroxyls (OH) with an apparent height of 0.8 Å (see also the Supporting Information). The O_{vac} surface density in the cluster-free surface areas is estimated to 12.5% ML (with respect to the density of the $TiO_2(110)$-(1 × 1) unit cells of 5.2 × 10^{14} cm^{-2}), which means that the surface of the TiO_2 crystal is strongly reduced.[53−56] The STM contrast on the $TiO_2(110)$ terraces is related to the empty states and well-known to be dominated by electronic effects.[53]

Figure 2a displays the CO_2 production on the surface shown in Figure 1 as a function of sample temperature when CO and O_2 reactants are pulsed alternatingly on the sample. To distinguish the product from CO_2 in the residual gas, we dose isotopic $^{13}C^{16}O$ (green) and $^{18}O_2$ (blue in the right insert in Figure 2a) and detect the yield of $^{13}C^{16}O^{18}O$. The flux of the CO_2 product is displayed in red when correlated with the CO pulse and in orange when correlated with the O_2 pulse (right insert in Figure 2a). This CO_2 production is very small. The CO_2 signal is composed of a temperature-independent background coming from the detector walls and a very small increase beyond this above 450 K. The CO_2 production is increased by more than an order of magnitude when this sample is sputtered with argon ions at room temperature and then annealed at 1100 K for 1 h (Supporting Information). As can be seen from comparison of the two STM images shown as insets in Figure 2, the morphology of the catalytically active sample is very similar to the one of the passive sample before the sputter−anneal treatment.

The CO_2 production as a function of temperature in Figure 2b —in particular, its correlation to O_2 at low and CO at high temperature—is reminiscent of Pt being the catalytically active element.[19] Note that Pd(111)[57−59] and Pd nanoclusters on MgO[60] display a similar behavior. The maximum of CO_2 production is observed at ∼470 K and estimated to 0.03 CO_2 per cluster surface Pt atom. This is ∼20 times higher than for the nonsputter-annealed Pt/TiO_2 sample (Figure 2a), estimated after subtraction of the CO_2 background measured at 300 K. It is synchronized with CO reacting with dissociated oxygen chemisorbed on the surfaces of the metal clusters. For temperatures between 370 and 450 K, we observe the coexistence of CO_2 production synchronized with the O_2 dosage. This is due to the oxidation of CO molecules chemisorbed on the clusters. This

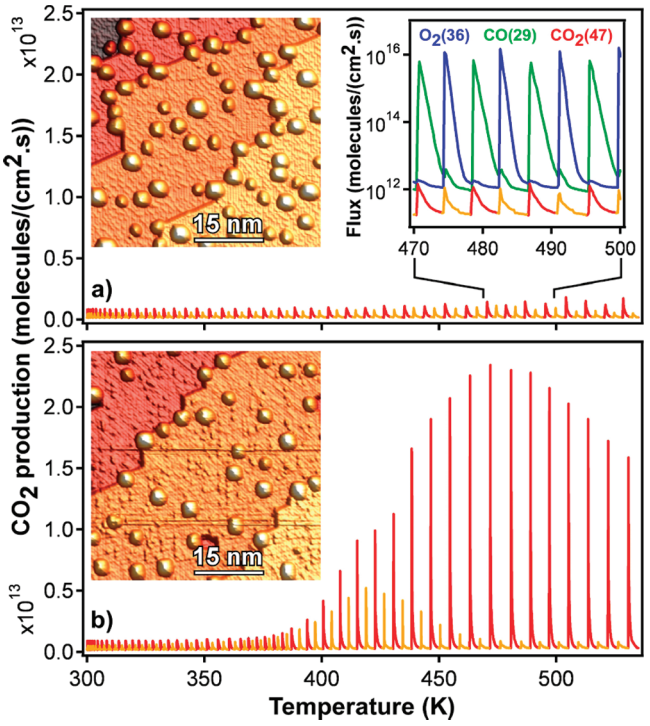

Figure 2. (a) Vanishingly small CO_2 production (red-orange) obtained on the SMSI sample displayed in the left inset upon dosing alternating pulses of O_2 (blue) and CO (green) as shown in the right inset as a function of the sample temperature and time (heating rate 1 K/s, pulse frequency 0.1 Hz). (b) High CO_2 production obtained on the sample displayed in the left inset (same preparation as in panel a), followed by Ar ion sputtering at room temperature and annealing at 1100 K for 1 h). Red and orange colors refer to the CO_2 production synchronized with CO and O_2 pulses, respectively.

CO_2 peak vanishes above 450 K, where CO desorbs and only oxygen remains adsorbed on the cluster surfaces. The fact that there is no CO_2 production beyond the background below 370 K is caused by the Pt clusters being fully covered by CO, leaving no surface sites for the dissociation of O_2 molecules, which is known as CO poisoning of the catalyst.[19,57−60]

A detailed analysis of the cluster morphology of the two differently prepared model catalysts (Figure 2) is presented in the apparent height histograms in Figure 3b and d derived from the STM images of Figure 3a and c, respectively. Both distributions show almost identical average apparent heights of 10.0 and 10.2 Å, respectively. The distributions are similar for large apparent heights; the small ones have a marked peak at 5.5 Å in Figure 3b that disappears in the activated sample (Figure 3d). We estimate the cluster volume from a half-sphere model for the clusters and from their surface densities of 2.7 × 10^{12} and 1.6 × 10^{12} cm^{-2} to be 35% and 19% ML, respectively, which is once above and once below the deposited amount of 25% ML Pt. Although this estimation has to be taken with care, it is indicative of the passive sample indeed presenting an encapsulation layer,[61] whereas this layer is absent—and probably some Pt has been sputtered away—in the active one. A further indication of the presence of a passivation layer in Figure 3a can be derived when attributing the prevailing apparent height of 5.5 Å to a monolayer of Pt covered by Ti suboxide,[61] which is much higher than a clean metal monolayer on TiO_2 (3.5 Å).[62,63] Figure 3 shows that both $Pt/TiO_2(110)$ samples have comparable cluster

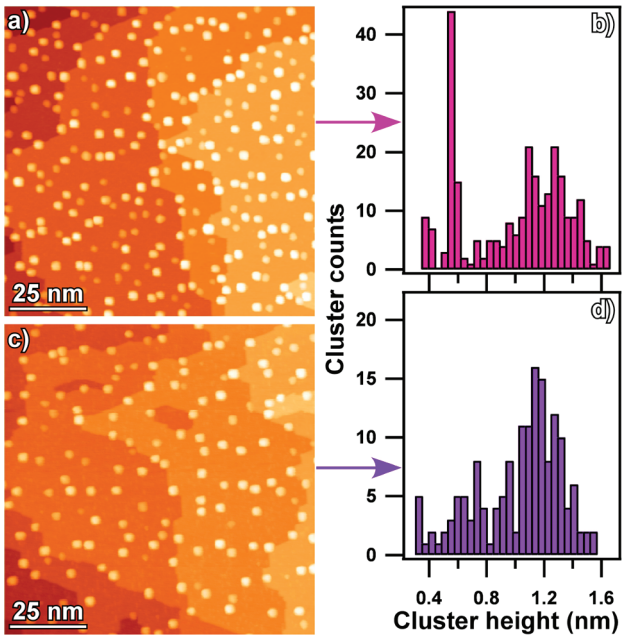

Figure 3. (a) Overview STM image of 25% ML Pt deposited at room temperature on $TiO_2(110)$-(1×1) followed by annealing at 1100 K over 3 h. (b) Apparent height distribution of the clusters observed in panel a. (c) Overview STM image of a $Pt/TiO_2(110)$ sample prepared as in panel a and followed by room temperature sputtering and annealing at 1100 K over 1 h. (d) Corresponding apparent height distribution.

sizes such that the large difference in the catalytic activity between the two samples (Figure 2) cannot be attributed to cluster size effects.

We attribute the very low catalytic activity in Figure 2a to the fact that the Pt clusters are encapsulated by a reduced titania layer that forms during the high-temperature treatment, as previously demonstrated and widely accepted in the SMSI literature.[22−50] The encapsulated clusters are characterized by a high thermal stability.[64] The encapsulating layer blocks the active sites of the Pt clusters and therefore passivates them toward the catalytic CO oxidation. The small CO_2 production observed in Figure 2a above 450 K may be caused by a few remaining active Pt sites because it is not observed on clean $TiO_2(110)$ surfaces and its behavior as a function of temperature is characteristic of Pt.

The mechanisms of metal encapsulation on oxides occurring in the SMSI state are complicated and not yet fully understood. One model has been proposed by Fu et al., who argued that the encapsulation is a multistep process and occurs only for metals with larger work function and surface energy as compared with those of the oxide support.[48,49] According to this model, metal encapsulation on TiO_2 requires (i) electron transfer from the oxide to the metal, (ii) the thermally activated outward diffusion of bulk Ti^{3+} interstitials, and finally, (iii) mass transport and migration of a thin oxide layer onto the surface of the metal, driven by a minimization of the surface energy of the system. The case of Pt on reduced $TiO_2(110)$ obeys all these criteria. Indeed, (i) the work function of Pt(111) is higher (by ~0.7 eV) than the one of $TiO_2(110)$,[48] and electron transfer from Ti^{3+} states of TiO_2-(110) to Pt atoms has been experimentally demonstrated.[65,66] In addition, (ii) the Ti^{3+} depletion from the bulk to the surface of $TiO_2(110)$ occurs for the same reasons as the widely studied oxygen-induced surface reconstruction.[53,56,67−70] Finally, (iii) the surface energy of Pt(111)[48,50] is about 5 times higher than that of $TiO_2(110)$.[71,72] These arguments, together with our reactivity measurements, strongly suggest that high-temperature annealing of Pt on reduced TiO_2 results in the encapsulation of Pt by a reduced titania layer.[33−42]

The high catalytic activity observed in Figure 2b results from sputter removal of the encapsulating suboxide layer from the SMSI Pt/TiO_2 sample. The surprising finding is that the encapsulating layer does not form again when the sputtered $Pt/TiO_2(110)$ sample is annealed to 1100 K. In addition to removing the encapsulation from the thermally stable Pt clusters,[64] ion sputtering also increases the reduction state of the cluster-free surface regions by preferentially depleting them of oxygen.[53] Annealing of oxygen-depleted TiO_2 surfaces above 700 K under ultrahigh vacuum restores the stoichiometry by the diffusion of Ti cations from the surface to the bulk of the crystal.[73] This is the case on Pt-free surface regions that appear in STM as clean $TiO_2(110)$-(1×1) with close to bulk stoichiometry (see Supporting Information). During the annealing of the sputtered sample to 1100 K, the diffusion direction of the Ti cations in the Pt-free surface regions is thus opposite to the one of the encapsulation process. In addition, the sputter-induced surface Ti cations diffuse into the bulk of the TiO_2 crystal rather than onto the Pt clusters.

We note that Rh and Pd particle encapsulation does occur if the metal is vapor-deposited on presputtered $TiO_2(110)$ surfaces that are then annealed to high temperatures.[32,48] This indicates that the absence of encapsulation in the case of our sputter-annealed $Pt/TiO_2(110)$ sample is due to the fact that the ion-sputtering treatment is performed after, not before, the clusters are formed and encapsulated. Due to the mechanisms outlined above occurring during the encapsulation, the interface between the metal clusters and the oxide support is expected to be modified by the encapsulation. This encapsulation-induced interface modification is a possible reason why the encapsulation process is self-limited to suboxide thicknesses of only one or two ML, as reported in the case of different metals on various oxide surfaces.[24−50] The self-limitation of the encapsulation is supported in our catalytic measurements by the small CO_2 production (Figure 2a) on the encapsulated Pt clusters, which likely still expose some active Pt sites at their surfaces, even after 3 h of heating at 1100 K. Therefore, one can understand that, if the suboxide layer encapsulating the metal clusters is removed, its reformation by subsequent high-temperature annealing is quenched. This gives rise to the highly active and thermally stable Pt clusters characterized in Figure 2b. In line with the metal-oxide-interface-based interpretation proposed here, we note that Nb doping of the near-surface region of TiO_2 also quenches the encapsulation of Pt during annealing.[50] To better understand the reasons for the metal encapsulation quenching, further investigations are necessary.

In conclusion, we have reported a sputter−anneal procedure that transfers Pt nanoclusters on $TiO_2(110)$-(1×1) from their almost inert SMSI state to a catalytically active and thermally stable one for CO oxidation. The procedure prevents the encapsulation of the Pt clusters by a thin, reduced titania layer, which usually forms by high-temperature treatment of Pt/TiO_2 and is known to be responsible for the catalytic passivity of the metal clusters. This procedure can in principle be applied to other (ultra)high-vacuum-prepared SMSI systems and to other catalytic reactions.

dx.doi.org/10.1021/cs200001y |*ACS Catal.* 2011, 1, 385–389

■ ASSOCIATED CONTENT

Supporting Information. Experimental details, STM images of the clean $TiO_2(110)$-(1×1) surface, catalytic CO oxidation on $Pt/TiO_2(110)$-(1×1) after deposition at room temperature, further STM images of $Pt/TiO_2(110)$, determination of the gas amounts, simulation of the CO oxidation. This material is available free of charge via the Internet at http://pubs.acs.org.

■ AUTHOR INFORMATION

Corresponding Author
*E-mail: kamel.ait-mansour@epfl.ch.

■ ACKNOWLEDGMENT

Financial support by the Swiss National Science Foundation is gratefully acknowledged. We thank Claude Henry and Hassan Sadeghi for helpful discussions.

■ REFERENCES

(1) Henry, C. R. *Surf. Sci. Rep.* **1998**, *31*, 231–325.
(2) Henry, C. R. *Prog. Surf. Sci.* **2005**, *80*, 92–116.
(3) Campbell, C. T. *Surf. Sci. Rep.* **1997**, *27*, 1–111.
(4) Cho, A. *Science* **2003**, *299*, 1684–1685.
(5) Haruta, M. *Catal. Today* **1997**, *36*, 153–166.
(6) Haruta, M.; Tsubota, S.; Kobayashi, T.; Kageyama, H.; Genet, M. J.; Delmon, B. *J. Catal.* **1993**, *144*, 175–192.
(7) Valden, M.; Lai, X.; Goodman, D. W. *Science* **1998**, *281*, 1647–1650.
(8) Choudhary, T. V.; Goodman, D. W. *Appl. Catal., A* **2005**, *291*, 32–36.
(9) Campbell, C. T. *Science* **2004**, *306*, 234–235.
(10) Lopez, N.; Nørskov, J. K. *J. Am. Chem. Soc.* **2002**, *124*, 11262–11263.
(11) Kim, T. S.; Stiehl, J. D.; Reeves, C. T.; Meyer, R. J.; Mullins, C. B. *J. Am. Chem. Soc.* **2003**, *125*, 2018–2019.
(12) Lee, S.; Fan, C.; Wu, T.; Anderson, S. L. *J. Am. Chem. Soc.* **2004**, *126*, 5682–5683.
(13) Lee, S.; Fan, C.; Wu, T.; Anderson, S. L. *J. Chem. Phys.* **2005**, *123*, 124710-1–124710-13.
(14) Lin, X.; Yang, B.; Benia, H.-M.; Myrach, P.; Yulikov, M.; Aumer, A.; Brown, M. A.; Sterrer, M.; Bondarchuk, O.; Kieseritzky, E.; Rocker, J.; Risse, T.; Gao, H.-J.; Nilius, N.; Freund, H.-J. *J. Am. Chem. Soc.* **2010**, *132*, 7745–7749.
(15) Sanchez, A.; Abbet, S.; Heiz, U.; Schneider, W.-D.; Ha1kkinen, H.; Barnett, R. N.; Landman, U. *J. Phys. Chem. A* **1999**, *103*, 9573–9578.
(16) Yoon, B.; Häkkinen, H.; Landman, U.; Wörz, A. S.; Antonietti, J.-M.; Abbet, S.; Judai, K.; Heiz, U. *Science* **2005**, *307*, 403–407.
(17) Arenz, M.; Landman, U.; Heiz, U. *ChemPhysChem* **2006**, *7*, 1871–1879.
(18) Roldán, A.; Ricart, J. M.; Illas, F.; Pacchioni, G. *J. Phys. Chem. C* **2010**, *114*, 16973–16978.
(19) Campbell, C. T.; Ertl, G.; Kuipers, H.; Segner, J. *J. Chem. Phys.* **1980**, *73*, 5862–5873.
(20) Wintterlin, J.; Völkening, S.; Janssens, T. V. W.; Zambelli, T.; Ertl, G. *Science* **1997**, *278*, 1931–1934.
(21) Tauster, S. J.; Fung, S. C.; Garten, R. L. *J. Am. Chem. Soc.* **1978**, *100*, 170–175.
(22) Tauster, S. J. *Acc. Chem. Res.* **1987**, *20*, 389–394.
(23) Haller, G. L.; Resasco, D. E. *Adv. Catal.* **1989**, *36*, 173–235.
(24) Sadeghi, H. R.; Henrich, V. E. *Appl. Surf. Sci.* **1984**, *19*, 330–340.
(25) Sadeghi, H. R.; Henrich, V. E. *J. Catal.* **1988**, *109*, 1–11.
(26) Bowker, M.; Stone, P.; Morrall, P.; Smith, R.; Bennett, R.; Perkins, N.; Kvon, R.; Pang, C.; Fourre, E.; Hall, M. *J. Catal.* **2005**, *234*, 172–181.
(27) Bowker, M.; Stone, P.; Bennett, R.; Perkins, N. *Surf. Sci.* **2002**, *497*, 155–165.
(28) Bowker, M.; Fourré, E. *Appl. Surf. Sci.* **2008**, *254*, 4225–4229.
(29) Bowker, M. *Phys. Chem. Chem. Phys.* **2007**, *9*, 3514–3521.
(30) Qin, Z.-H.; Lewandowski, M.; Sun, Y.-N.; Shaikhutdinov, S.; Freund, H.-J. *J. Phys. Chem. C* **2008**, *112*, 10209–10213.
(31) Qin, Z.-H.; Lewandowski, M.; Sun, Y.-N.; Shaikhutdinov, S.; Freund, H.-J. *J. Phys.: Condens. Matter* **2009**, *21*, 134019-1–134019-6.
(32) Berkó, A.; Ulrych, I.; Prince, K. C. *J. Phys. Chem. B* **1998**, *102*, 3379–3386.
(33) Dulub, O.; Hebenstreit, W.; Diebold, U. *Phys. Rev. Lett.* **2000**, *84*, 3646–3649.
(34) Jennison, D. R.; Dulub, O.; Hebenstreit, W.; Diebold, U. *Surf. Sci.* **2001**, *492*, L677–L687.
(35) Belton, D. N.; Sun, Y.-M.; White, J. M. *J. Phys. Chem.* **1984**, *88*, 5172–5176.
(36) Sun, Y.-M.; Belton, D. N.; White, J. M. *J. Phys. Chem.* **1986**, *90*, 5178–5182.
(37) Pesty, F.; Steinrück, H.-P.; Madey, T. E. *Surf. Sci.* **1995**, *339*, 83–95.
(38) Haller, G. L. *J. Catal.* **2003**, *216*, 12–22.
(39) Park, J. B.; Ratliff, J. S.; Ma, S.; Chen, D. A. *J. Phys. Chem. C* **2007**, *111*, 2165–2176.
(40) Park, J. B.; Conner, S. F.; Chen, D. A. *J. Phys. Chem. C* **2008**, *112*, 5490–5500.
(41) Ozturk, O.; Park, J. B.; Ma, S.; Ratliff, J. S.; Zhou, J.; Mullins, D. R.; Chen, D. A. *Surf. Sci.* **2007**, *601*, 3099–3113.
(42) Bardi, U.; Tamura, K.; Nihei, Y. *Catal. Lett.* **1989**, *3*, 117–128.
(43) Sadeghi, H. R.; Henrich, V. E. *J. Catal.* **1984**, *87*, 279–282.
(44) Bennett, R. A.; Pang, C. L.; Perkins, N.; Smith, R. D.; Morrall, P.; Kvon, R. I.; Bowker, M. *J. Phys. Chem. B* **2002**, *106*, 4688–4696.
(45) Bennett, R. A.; Stone, P.; Bowker, M. *Catal. Lett.* **1999**, *59*, 99–105.
(46) Bernal, S.; Calvino, J. J.; Cauqui, M. A.; Gatica, J. M.; López Cartes, C.; Pérez Omil, J. A.; Pintado, J. M. *Catal. Today* **2003**, *77*, 385–406.
(47) Zhou, Y.; Perket, J. M.; Zhou, J. *J. Phys. Chem. C* **2010**, *114*, 11853–11860.
(48) Fu, Q.; Wagner, T.; Olliges, S.; Carstanjen, H.-D. *J. Phys. Chem. B* **2005**, *109*, 944–951.
(49) Fu, Q.; Wagner, T. *Surf. Sci. Rep.* **2007**, *62*, 431–498.
(50) Gao, Y.; Liang, Y.; Chambers, S. A. *Surf. Sci.* **1996**, *365*, 638–648.
(51) Jödicke, H.; Schaub, R.; Bhowmick, A.; Monot, R.; Buttet, J.; Harbich, W. *Rev. Sci. Instrum.* **2000**, *71*, 2818–2828; see also Bonanni, S.; Aït-Mansour, K.; Hugentobler, M.; Brune, H.; Harbich, W. *Eur. Phys. J. D*, in press.
(52) All STM images have been measured in the constant-current mode (sample bias = +1.5 V, tunneling current = 0.1 nA) at a sample temperature of 80 K, and they have been processed with the WSxM software: Horcas, I.; Fernández, R.; Gómez-Rodríguez, J. M.; Colchero, J.; Gómez-Herrero, J.; Baro, A. M. *Rev. Sci. Instrum.* **2007**, *78*, 013705-1–013705-8.
(53) Diebold, U. *Surf. Sci. Rep.* **2003**, *48*, 53–229 and references therein.
(54) Wendt, S.; Sprunger, P. T.; Lira, E.; Madsen, G. K. H.; Li, Z.; Hansen, J. Ø.; Matthiesen, J.; Blekinge-Rasmussen, A.; Lægsgaard, E.; Hammer, B.; Besenbacher, F. *Science* **2008**, *320*, 1755–1759.
(55) Yim, C. M.; Pang, C. L.; Thornton, G. *Phys. Rev. Lett.* **2010**, *104*, 036806-1–036806-4.
(56) Zhang, Z.; Lee, J.; Yates, J. T., Jr.; Bechstein, R.; Lira, E.; Hansen, J. Ø.; Wendt, S.; Besenbacher, F. *J. Phys. Chem. C* **2010**, *114*, 3059–3062.
(57) Engel, T.; Ertl, G. *Chem. Phys. Lett.* **1978**, *54*, 95–98.
(58) Engel, T.; Ertl, G. *J. Chem. Phys.* **1978**, *69*, 1267–1281.

(59) Conrad, H.; Ertl, G.; Küppers, J. *Surf. Sci.* **1978**, *76*, 323.
(60) Kunz, S.; Schweinberger, F. F.; Habibpour, V.; Röttgen, M.; Harding, C.; Arenz, M.; Heiz, U. *J. Phys. Chem. C* **2010**, *114*, 1651–1654.
(61) Sedona, F.; Rizzi, G. A.; Agnoli, S.; Llabrés i Xamena, F. X.; Papageorgiou, A.; Ostermann, D.; Sambi, M.; Finetti, P.; Schierbaum, K.; Granozzi, G. *J. Phys. Chem. B* **2005**, *109*, 24411–24426.
(62) Isomura, N.; Wu, X.; Watanabe, Y. *J. Chem. Phys.* **2009**, *131*, 164707-1–164707-4.
(63) Isomura, N.; Wu, X.; Hirata, H.; Watanabe, Y. *J. Vac. Sci. Technol. A* **2010**, *28*, 1141–1144.
(64) Naitabdi, A.; Behafarid, F.; Roldan Cuenya, B. *Appl. Phys. Lett.* **2009**, *94*, 083102-1–083102-3.
(65) Schierbaum, K. D.; Fischer, S.; Torquemada, M. C.; de Segovia, J. L.; Román, E.; Martín-Gago, J. A. *Surf. Sci.* **1996**, *345*, 261–273.
(66) Fischer, S.; Schneider, F.; Schierbaum, K. D. *Vacuum* **1996**, *47*, 1149–1152.
(67) Onishi, H.; Iwasawa, Y. *Phys. Rev. Lett.* **1996**, *76*, 791–794.
(68) Onishi, H.; Iwasawa, Y. *Surf. Sci.* **1994**, *313*, L783–L789.
(69) Bennett, R. A.; Stone, P.; Price, N. J.; Bowker, M. *Phys. Rev. Lett.* **1999**, *82*, 3831–3834.
(70) Li, M.; Hebenstreit, W.; Gross, L.; Diebold, U.; Henderson, M. A.; Jennison, D. R.; Schultz, P. A.; Sears, M. P. *Surf. Sci.* **1999**, *437*, 173–190.
(71) Kiejna, A.; Pabisiak, T.; Gao, S. W. *J. Phys.: Condens. Matter* **2006**, *18*, 4207–4217.
(72) Harris, L. A.; Quong, A. A. *Phys. Rev. Lett.* **2004**, *93*, 086105-1–086105-4.
(73) Henderson, M. A. *Surf. Sci.* **1999**, *419*, 174–187.